energies

MDPI

Article

Energy Demand Modeling Methodology of Key State Transitions of Turning Processes

Shun Jia [1,*], Qinghe Yuan [1,*], Dawei Ren [1] and Jingxiang Lv [2]

[1] Department of Industrial Engineering, Shandong University of Science and Technology, Qingdao 266590, China; dawei_ren_2000@163.com

[2] Key Laboratory of Contemporary Design and Integrated Manufacturing Technology, Ministry of Education, Northwestern Polytechnical University, Xi'an 710072, China; youyilong@zju.edu.cn

* Correspondence: herojiashun@163.com (S.J.); yuan_qinghe@sina.com (Q.Y.); Tel.: +86-532-8605-7044 (S.J.)

Academic Editor: Rick Greenough

Received: 5 January 2017; Accepted: 24 March 2017; Published: 2 April 2017

Abstract: Energy demand modeling of machining processes is the foundation of energy optimization. Energy demand of machining state transition is integral to the energy requirements of the machining process. However, research focus on energy modeling of state transition is scarce. To fill this gap, an energy demand modeling methodology of key state transitions of the turning process is proposed. The establishment of an energy demand model of state transition could improve the accuracy of the energy model of the machining process, which also provides an accurate model and reliable data for energy optimization of the machining process. Finally, case studies were conducted on a CK6153*i* CNC lathe, the results demonstrating that predictive accuracy with the proposed method is generally above 90% for the state transition cases.

Keywords: turning process; state transition; energy modeling; sustainable manufacturing

1. Introduction

The report of the International Energy Agency (IEA) revealed that nearly one-third of global energy use and 40% of carbon dioxide (CO_2) emissions are attributable to the manufacturing industry [1]. It is evident that the manufacturing industry has become one of the major sources of energy consumption and CO_2 emissions, which will continue to increase by 1.9% annually if no effective action is taken [2]. Improved industrial energy efficiency is a critical cornerstone in climate change mitigation [3]. Therefore, the manufacturing industry must take responsibility and strive to adopt more energy-efficient and sustainable production techniques [4]. If energy data and information can be more effectively used and analyzed in manufacturing, it will provide considerable insights into energy-saving opportunities [5]. The machining process, as one of the major processes of manufacturing industries [6], is vital to energy saving and emission reduction. Generally, the life cycle of a product can be divided into several stages: material production; manufacture and assembly; transport; use; and end-of-life. Machine tools follow the same pattern and its Life Cycle Analysis (LCA) has shown that 95% of the environmental impact of a machine tool is associated with its use phase (assuming a 10-year lifespan). Of that use phase impact, 95% comes from energy consumption [7]. However, because the life cycle of a machine tool is usually more than 15 years, even reaching up to 20 years (with the current trends indicating that the industry will most likely want to prolong their lifecycle) [8,9], the environmental impact from the use phase of machine tools tends to be greater than 95%, even going as high to 99%. Similar results in another study [10] have shown that CO_2 emissions caused by the energy consumption of a computer numerical control (CNC) machine tool (spindle power is 22 kW) over one year was equivalent to the CO_2 emissions of 61 SUVs.

It thus becomes clear that the energy consumption and emissions derived from the machining process is very significant. Triggered by the necessity to improve the energy efficiency and environmental performance of the manufacturing industry, energy modeling [11–16], energy-efficiency improvement [17–22] and carbon-emission reduction [23,24] of the manufacturing industry have been studied. Experiments show that power peaks will be caused by state transitions during the machining process [25,26], as shown in Figure 1. State transition indicates the transition process between the two neighboring states during the machining process, such as spindle startup, rapid positioning acceleration, coolant startup, tool change startup, etc. State transition generally relates to the instantaneous startup of the motor, as well as the instant momentum through increase of torque or moving parts, etc., which result in power increase and the subsequent phenomenon of peak power. However, intensive research about energy consumption characteristics and models of state transitions is scarce. To fill this gap, an energy demand modeling method for state transition of the turning process is proposed in this paper.

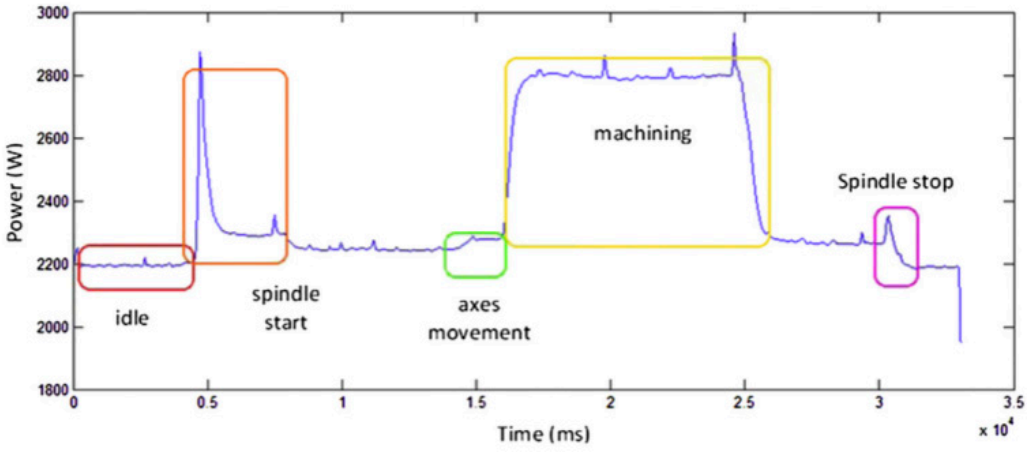

Figure 1. Power curve during an actual machining process [25].

The peak power caused by machining state transition has been mentioned in many references [25–27]. However, the mechanism and energy demand model of the power peak has not been researched in depth; the existing studies have only demonstrated the phenomenon of peak power in the power curve. The duration of state transition is short, but the peak power caused by the state transition is high [27,28], making the energy demand of the state transitions significant. Moreover, state transitions occur frequently during the machining processes. The energy demand of state transition was not considered in reference [29]; therefore, the predicted energy is 9.3% less than the measured energy in the machining case. It can be observed that the energy demand of state transition is a vital part of the energy demand of the entire machining process.

Although the power peak of the spindle startup was measured in the literature [30], its energy demand was not. The spindle and feed axis acceleration power models were studied based on the torque and angular velocity [31]; however, the friction torque and the torque for overcoming the spindle rotational inertia involved in the models are very difficult to obtain, making the established models difficult to apply in real machining cases. Shi et al. measured the energy consumption of spindle from stopping state to different speeds and obtained the spindle startup energy model through quadratic function fitting [32]; the established model can be used to calculate the spindle startup energy from stopping to the specified speed. When the initial spindle speed is not zero (accelerating from low speed to high speed), the above model will not be applicable. Moreover, as shown in the energy supply model of the spindle startup established in our previous work [33], the model can only calculate the energy consumption of the spindle system during spindle speedup. However, during the spindle speedup process, standby operation, X,Y,Z-axis feeding, chip conveying, cutting flood spraying and

other motions can also be executed. The actual energy demand of the spindle speedup is the sum of the energy demand of all the listed motions. Whether those motions are executed or not during spindle speed-up is dependent on the operating status of the machine tool. The operation status of a machine tool is strongly dynamic; only when determining the operating status of a machine tool during the spindle speedup can we accurately calculate the total energy demand of the spindle speedup process.

In summary, although the durations of machining state transitions are short, the power peak caused by the state transition is high and its energy demand cannot be ignored. Most of the abovementioned references have shown the peak power phenomenon to be caused by the state transition, but the quantitative analysis of the energy demand of state transition is lacking. To fill this gap, an energy demand modeling methodology of key state transition of the turning processes is proposed in this paper, which can further be applied to the evaluation and optimization of energy demand of the machining process and provide theoretical support for low-carbon manufacturing.

2. State Transition Classification Based on Energy Demand

The framework of the proposed methodology is shown in Figure 2. Firstly, the Pareto chart of energy demands of state transitions for the turning process is developed. Then, key state transitions and non-key state transitions are classified according to the established Pareto chart. For the identified key state transitions (supposing F, D, B are determined as the key state transitions), energy demand characteristics are researched and the energy demand model for each type of key state transition is established. Finally, the experimental studies and case studies will be conducted to validate the proposed energy demand model of the key state transition of the turning process. The state transition classification and the identification of the key state transitions are the first step for energy demand modeling of state transitions, which is discussed in this section.

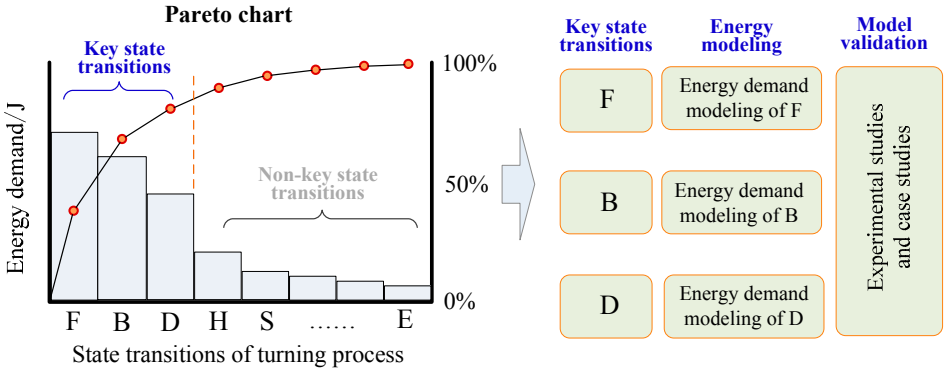

Figure 2. Framework of the proposed methodology.

The common state transition is summarized as follows: machine tool (off→on), machine tool (on→off), lighting (off→on), lighting (on→off), cooling (off→on), cooling (on→off), chip conveying (off→on), chip conveying (on→off), spindle rotation (Ls→Hs), spindle rotation (Hs→Ls), positioning (Ls→Hs), positioning (Hs→Ls), tool changing (off→on), tool changing (on→off), material cutting (off→on), material cutting (on→off). More specifically, (off→on) indicates the state transitions from "off" mode to "on" mode; (on→off) indicates the state transitions from "on" mode to "off" mode. Similarly, (Ls→Hs) means the state transitions from "Low speed" mode to "High speed" mode; (Hs→Ls) means the state transitions from "High speed" mode to "Low speed" mode. Energy demand of each state transition is analyzed by means of experiment and the key state transitions are identified according to the Pareto principle. Taking CK6153*i* CNC lathe as an example, the energy demand of each state transition can be obtained by using the power and energy acquisition experimental device built by our research group [12]. The experimental device is composed of three current sensors, three voltage sensors, two NI-9215 data acquisition cards and one compact DAQ crate, etc. The experimental

device is connected to the main power box of the CK6153*i* CNC lathe. Moreover, the power and energy information is measured and stored in the Server SQL database for offline analysis. For more information about the experimental device, you can refer to Figure 10 in Section 4. The energy demands of chip conveying (off→on) and lighting (off→on) are the estimated values because the machine tool mentioned above does not have an automatic chip conveying device and the lighting device cannot be controlled separately. In addition, because the state transition lighting/cooling/chip conveying/tool changing/machine tools (on→off) only involve instant closing of motor or lighting device, the energy demand is very low, at a value of around 5 J. The Pareto chart is obtained according to the energy demand value of each state transition gained by actual measurement, as shown in Figure 3.

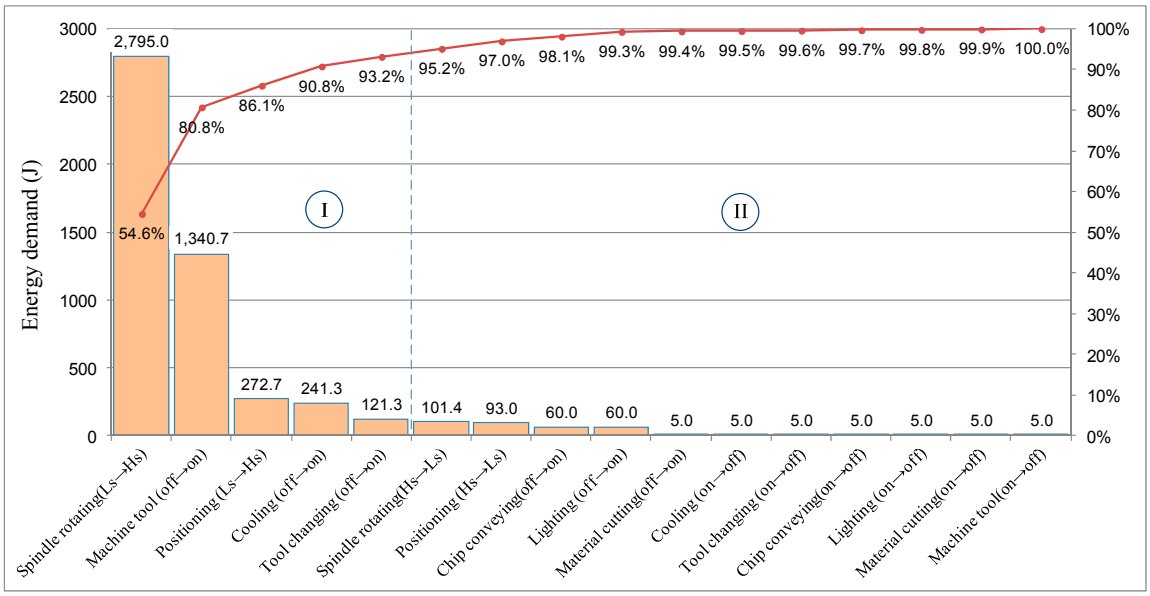

Figure 3. Pareto chart during an actual turning process.

According to the above Pareto chart and in accordance with the 80/20 rule, the top 20% of state transitions (top four transitions) ranked by energy demands are determined as key state transitions. The machine tool (off→on) includes three manually operated sub-movements: starting the air switch, starting the numerical control (NC) control panel, and releasing the emergency stop button. The energy demand of the machine tool (off→on) is the sum of energy demand caused by these three sub-movements. Because they are manually operated, however, the duration of the machine tool (off→on) depends on the operators. Accurate energy demand (off→on) is difficult to be obtain and therefore does not fall within the scope of this manuscript. Hence, spindle rotation (Ls→Hs), positioning (Ls→Hs), cooling (off→on) and tool changing (off→on) are finally determined to be the key state transitions (Category I), whereas other state transitions are non-key (Category II). It can be seen from the Pareto chart that the energy demand of key state transitions accounts for over 80% of the total energy demand of state transitions, thus warranting further study.

3. Methodology

3.1. Energy Demand Model of Spindle Rotation (Ls→Hs)

Spindle rotation (Ls→Hs) is the transfer process of the spindle accelerating from low speed (minimum is 0 r/min) to high speed under the conditions of non-cutting loading. Figure 4 shows the power curves of spindle rotation (Ls→Hs) (initial speed n_1 = 0 r/min, the target speed n_2 = 750 r/min) of CK6153*i* CNC lathes. Energy demand of state transition spindle rotation (Ls→Hs) includes not only energy demand of the spindle system itself, but also energy demand of supporting therbligs

(standby operating, lighting, etc.) during this state transition. Energy demand of spindle rotation (Ls→Hs) consists of three parts: (1) Energy demand of spindle system from spindle rotation start to peak power (E_{SR1}); (2) Energy demand of spindle system from peak power to stable power (E_{SR2}); (3) Energy demand of supporting therbligs during spindle rotation (Ls→Hs) (E_{SR3}). Thus, the energy demand of state transition of spindle rotation (Ls→Hs) is written as:

$$E_{SRA} = E_{SR1} + E_{SR2} + E_{SR3} \tag{1}$$

where E_{SRA} is energy demand of spindle rotation(Ls→Hs), J.

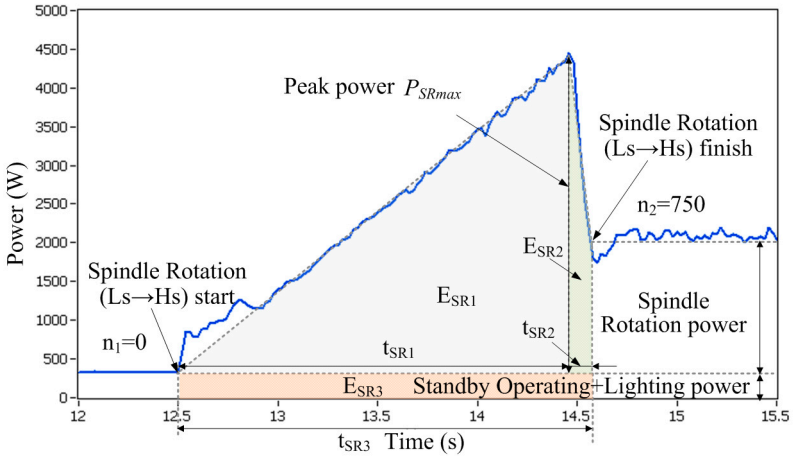

Figure 4. Power curve of spindle rotation (Ls→Hs).

The energy demand of the spindle system from spindle rotation start to peak power (E_{SR1}) is calculated as:

$$E_{SR1} = \int_0^{t_{SR1}} P_{SR1}\, dt \tag{2}$$

where P_{SR1} is the power of the spindle system from spindle rotation start to peak power, W; t_{SR1} is duration from spindle rotation start to peak power, s.

The power of the spindle system during the acceleration process is further expressed as [33]:

$$P_{SR1} = P_{SR}(n) + T_s\omega_s = P_{SR}\left(n_1 + 30\alpha t/\pi\right) + T_s\left(\pi n_1/30 + \alpha t\right) \tag{3}$$

The theoretical derivation process of P_{SR1} is shown in Figure 5. Hence, the developed equation model has a certain degree of versatility.

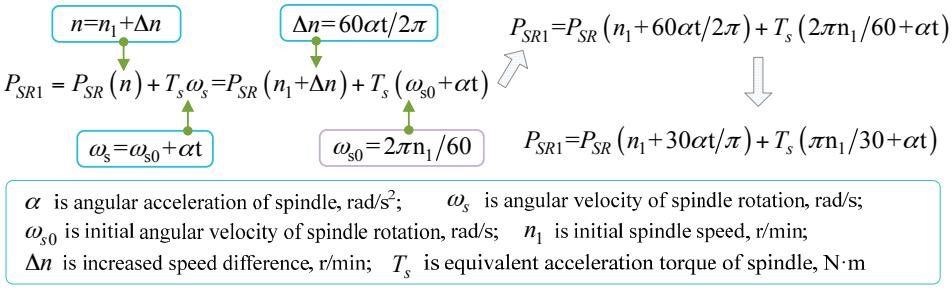

Figure 5. Theoretical derivation process of P_{SR1}.

The developed model contains some machine tool design and electrical control-related parameters (equivalent acceleration torque of spindle T_s, etc.). However, the machine manual usually provides machine configuration-, operation- and maintenance-related information; descriptions of design and electrical control-related parameters are very limited (for technical protection reasons). Consequently, some coefficients of the developed model is difficult to be obtained without experiments, which hinder the application of the model. To make the model easier to use, the coefficients of the model (equivalent acceleration torque of spindle-T_s, angular acceleration of spindle-α, etc.) can be obtained based on the experimental studies. More specifically, each obtained coefficient value was the average value of multiple measurements. Once the coefficients of the energy model of state transitions for one machine tool are obtained, these models can be used for a long period of time. When it comes to another machine tool (of the same type of), the formula form of the energy model of state transitions can be adopted, though the coefficient values need to be updated with several simple experimental measurements.

The duration from spindle rotation start to peak power t_{SR1} is calculated as:

$$t_{SR1} = \frac{2\pi(n_2 - n_1)}{60\alpha} \tag{4}$$

where n_1 is initial spindle speed, r/min; n_2 is target spindle speed, r/min; α is angular acceleration of spindle, rad/s^2.

The energy demand of spindle system E_{SR2} from peak power to stable power is written as

$$E_{SR2} = \frac{P_{SRmax} + P_{SR}(n_2)}{2} t_{SR2} \tag{5}$$

where P_{SRmax} is power peak of spindle speedup, W; P_{SR} is the spindle power, W; n_2 is target spindle speed, r/min; t_{SR2} is the duration from peak power to stable power, s. t_{SR2} can be obtained based on experimental measurement combined with statistical analysis.

The power peak of spindle speedup (P_{SRmax}) is spindle accelerating power at the moment (t_{SR1}). According to Equation (3), the peak power of spindle speedup is expressed as:

$$P_{SRmax} = P_{SR1}(t_{SR1}) = P_{SR}\left(n_1 + 30\alpha t_{SR1}/\pi\right) + T_s\left(\pi n_1/30 + \alpha t_{SR1}\right) \tag{6}$$

The energy demand of supporting therbligs during spindle rotation (Ls→Hs) is relevant to the type and quantity of supporting therblig during state transition and the status of supporting therblig is judged by the state vector in forward-operating state [34]. The value 1 in state vector is reflected as the supporting therblig. The energy demand of supporting therbligs during spindle rotation (Ls→Hs) (E_{SR3}) is calculated as:

$$E_{SR3} = \int_0^{t_{SR3}} \vec{OP} \cdot \vec{OS}\, dt \tag{7}$$

where $\vec{OP}$ is the power vector of forward-operating state; $\vec{OS}$ is the state vector of forward-operating state; t_{SR3} is the duration of spindle rotation (Ls→Hs), s. The detail explanations of Equation (7) are shown in Figure 6. $s_1 \sim s_{11}$ are the logical representations for these eleven types of therbligs, which are represented by 0–1 variables. More specifically, when the supporting therblig is executed, then s = 1 can be obtained; otherwise, s = 0 is obtained. For instance, supposing only the therblig-standby operating and therblig-lighting are executed, then $s_1 = s_2 = 1$ can be obtained, and $s_3 \sim s_{11}$ are all set to be 0. As a result, the power of supporting therbligs can be expressed as: $\vec{OP} \cdot \vec{OS} = P_{SO} \cdot 1 + P_L \cdot 1 + P_{CFS} \cdot 0 + \ldots + P_{MC} \cdot 0 = P_{SO} + P_L$. The power model and calculation approach have been researched in our previous work [34].

The energy demand of supporting therbligs during the state transition process (E_{SR3}) is further calculated as:

$$E_{SR3} = \int_0^{t_{SR3}} \left[P_{SO} \cdot s_1 + P_L \cdot s_2 + P_{CFS} \cdot s_3 + \ldots + P_{MC} \cdot s_{11} \right] dt \quad (8)$$

The duration of spindle rotation (Ls→Hs) t_{SR3} is calculated as:

$$t_{SR3} = t_{SR1} + t_{SR2} \quad (9)$$

where t_{SR1} is duration from spindle rotation start to peak power, s; t_{SR2} is duration from peak power to stable power, s.

Substituting the Formulas (2)–(8) into Equation (1) to get the energy demand of spindle rotation (Ls→Hs):

$$\begin{aligned} E_{SRA} = & \int_0^{t_{SR1}} \left[P_{SR}\left(n_1 + 30\alpha t/\pi\right) + T_s(\pi n_1/30 + \alpha t) \right] dt \\ & + 0.5\left[P_{SR}\left(n_1 + 30\alpha t_{SR1}/\pi\right) + T_s\left(\pi n_1/30 + \alpha t_{SR1}\right) + P_{SR}\left(n_2\right) \right] t_{SR2} \\ & + \int_0^{t_{SR3}} \left[P_{SO} \cdot s_1 + P_L \cdot s_2 + P_{CFS} \cdot s_3 + \ldots + P_C \cdot s_{11} \right] dt \end{aligned} \quad (10)$$

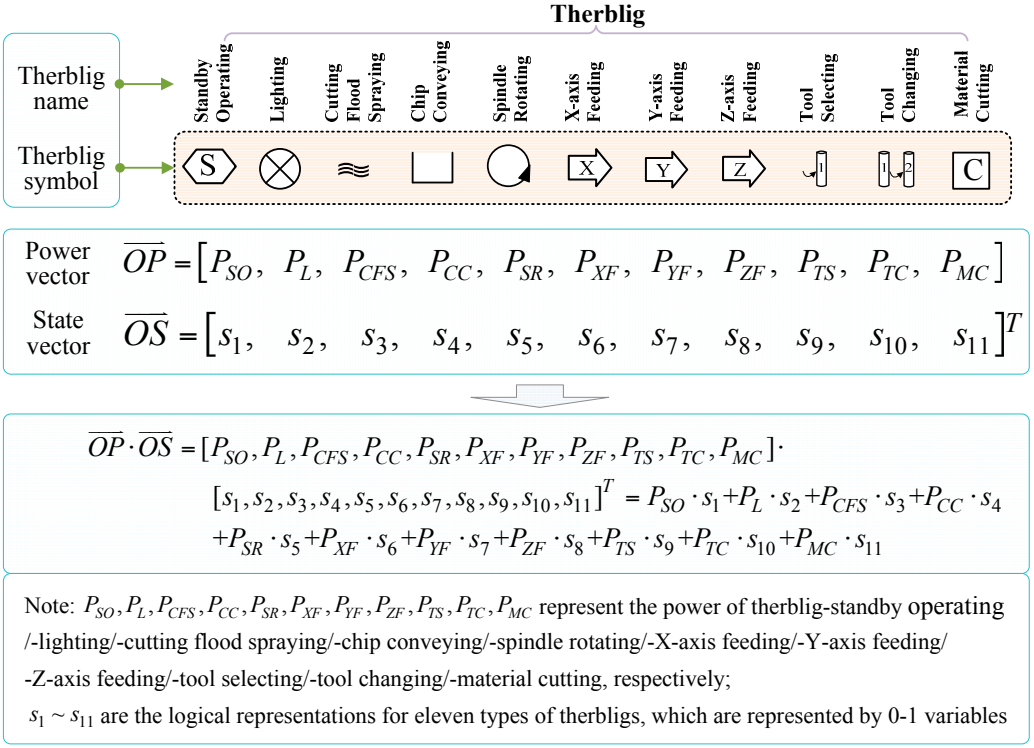

Figure 6. Detail explanations of Equation (7).

3.2. Energy Demand Model of Positioning (Ls→Hs)

Positioning (Ls→Hs) is the transfer process of feeding system from low feeding speed (minimum is 0 r/min) to the maximum feeding speed. For a given feeding system, the maximum feed speed of each axis is definite. Taking CK6153*i* lathe as an example, the maximum feed speed of X-axis is 6 m/min and maximum feed speed of Z-axis is 10 m/min [35]. Figure 7 shows the power curve of Z-axis positioning (Ls→Hs) of CNC CK6153*i* lathe (initial feed speed v_{f0} = 0 mm/min, maximum feed rate v_{f1} = 10,000 mm/min). Similar to the state transition spindle rotation (Ls→Hs), energy

demand of positioning (Ls→Hs) includes not only energy demand of the feeding system itself, but also energy demand of supporting therbligs (standby operating, lighting, etc.) during this state transition. Hence, the energy demand of positioning (Ls→Hs) consists of two parts: (1) Energy demand of feeding system during positioning (Ls→Hs) (E_{F1}); (2) Energy demand of supporting therblig during positioning (Ls→Hs) (E_{F2}). Thus, energy demand of positioning (Ls→Hs) is calculated as:

$$E_{FA} = E_{F1} + E_{F2} \tag{11}$$

where E_{FA} is the energy demand of positioning (Ls→Hs), J.

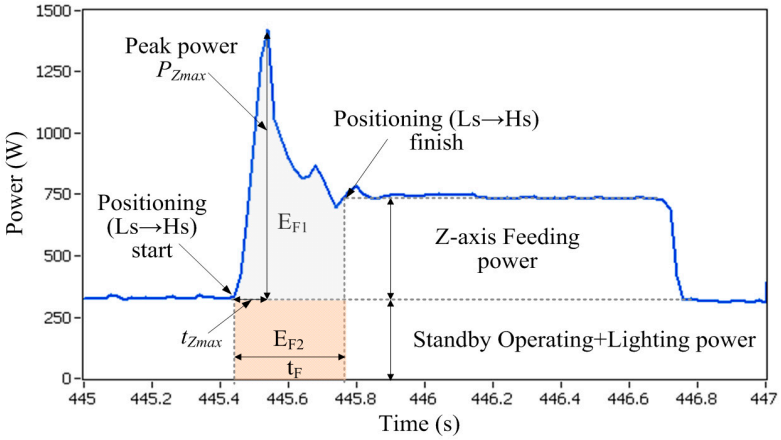

Figure 7. Power curve of positioning (Ls→Hs).

Generally, the rapid positioning accelerations of each axis of a CNC machine is very large, some being more than 1 g [36]. Therefore, the duration of positioning (Ls→Hs) is very short, although it can cause large power peaks (corresponding to the maximum feed speed). For each feed axis, there is a critical feeding distance L_{f0}. When the feeding distance is $L_f < L_{f0}$, the feeding axis begins deceleration before reaching the maximum feeding speed. Because the power peak does not reach the maximum value, the duration of positioning (Ls→Hs) is very short, subsequently leading to the low energy demand in this condition. Therefore, when the feeding distance is $L_f < L_{f0}$, energy demand of positioning (Ls→Hs) is negligible. When the feeding distance is $L_f \geq L_{f0}$, the feed axis can accelerate to the maximum speed and the corresponding power reaches a maximum power peak. Therefore, this subsection focuses on the energy demand of positioning (Ls→Hs) when feeding distance is $L_f \geq L_{f0}$.

The critical feeding distance L_{f0} can be expressed as [33]:

$$L_{f0} = \frac{v_{rmax}^2}{7200 a_f} + \frac{v_{rmax}^2}{7200 d_f} \tag{12}$$

where v_{rmax} is the maximum feeding speed of feed table, mm/min; a_f is acceleration in feed table, mm/s^2; d_f is deceleration of feed table, mm/s^2. v_{rmax} can be obtained from the machine manual a_f and d_f can be calculated according to the machine design information.

The energy demand of feeding system during positioning (Ls→Hs) E_{F1} is calculated as:

$$E_{F1} = \int_0^{t_F} P_{F1}(t)\, dt \tag{13}$$

where $P_{F1}(t)$ is power function of feeding system during positioning (Ls→Hs).

For a given feeding system, the maximum feeding speed v_{rmax} and feeding acceleration a_f of positioning (Ls→Hs) is definite, and the initial feed rate of positioning (Ls→Hs) is 0 mm/min. Hence, for each feed axis, when the feeding distance is $L_f \geq L_{f0}$, the energy demand of feeding system E_{F1} and

transfer time t_F of positioning (Ls→Hs) are definite values, which can be obtained by experimental measurements combined with statistical analysis.

The supporting therbligs during positioning (Ls→Hs) need to be judged by the state vector in the forward-operating state [34]. The value 1 in the state vector is reflected as the supporting therblig. The energy demand of the supporting therblig (E_{F2}) during positioning (Ls→Hs) is calculated as:

$$E_{F2} = \int_0^{t_F} \left[P_{SO} \cdot s_1 + P_L \cdot s_2 + P_{CFS} \cdot s_3 + \ldots + P_C \cdot s_{11} \right] dt \tag{14}$$

where t_F is the duration of positioning (Ls→Hs), s.

The energy demand of positioning (Ls→Hs) is obtained by substituting the Formula (13) and (14) into Formula (11)

$$E_{FA} = \int_0^{t_F} P_{F1}(t)\, dt + \int_0^{t_F} \left[P_{SO} \cdot s_1 + P_L \cdot s_2 + P_{CFS} \cdot s_3 + \ldots + P_C \cdot s_{11} \right] dt \tag{15}$$

3.3. Energy Demand Model of Cooling (off→on)

Cooling (off→on) means the transfer process of the cooling device from "off" state to "power on" state. The energy demand of this state transition includes not only energy demand of the cooling device itself, but also energy demand of supporting therbligs (standby operating, lighting, etc.) during the state transition. Figure 8 shows a power curve of the cooling (off→on) process for the CK6153*i* CNC lathe. Energy demand of cooling (off→on) includes two parts: (1) Energy demand of cooling device during cooling (off→on) (E_{CF1}); (2) Energy demand of supporting therblig during cooling (off→on) (E_{CF2}). Therefore, the energy demand of cooling (off→on) can be calculated as:

$$E_{CFA} = E_{CF1} + E_{CF2} \tag{16}$$

where E_{CFA} is the energy demand of cooling (off→on), J.

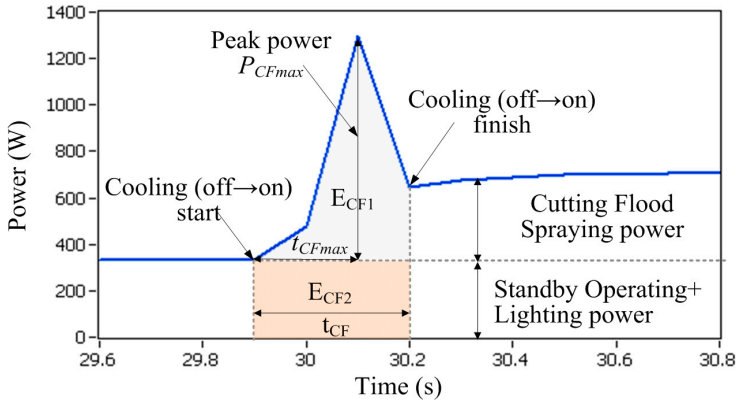

Figure 8. Power curve of cooling (off→on).

For a given CNC machine tool, energy demand of the cooling system (E_{CF1}) and transfer time of the cooling (off→on) process (t_{CF}) are stable values, which can be obtained by experimental measurement combined with statistical analysis.

The supporting therbligs during cooling (off→on) need to be judged by the state vector in the forward-operating state. The value 1 in the state vector is reflected as the supporting therblig. The energy demand of supporting therbligs during cooling (off→on) (E_{CF2}) is calculated as:

$$E_{CF2} = \int_0^{t_{CF}} \left[P_{SO} \cdot s_1 + P_L \cdot s_2 + P_{CFS} \cdot s_3 + \ldots + P_C \cdot s_{11} \right] dt \tag{17}$$

where t_F is the duration of cooling (off→on) process, s.

The energy demand of cooling (off→on) can be obtained by substituting the Formula (17) into (16).

$$E_{CFA} = E_{CF1} + \int_0^{t_{CF}} \left[P_{SO} \cdot s_1 + P_L \cdot s_2 + P_{CFS} \cdot s_3 + \ldots + P_C \cdot s_{11} \right] dt \tag{18}$$

3.4. Energy Demand Model of Tool Changing (off→on)

Tool changing (off→on) is the transfer process of a tool device changing from "off" state to "steady power" state. Figure 9 shows an actual power curve of tool changing (off→on) of CK6153*i* CNC lathe. It can be seen that several power peaks occur in the power curve. The reason is that the tool changing (off→on) process includes several sub-actions, such as tool changing motor rotating startup, turret rotation and motor braking. In this paper, the energy demand of tool changing (off→on) is viewed as the sum of energy demand of power peak caused by the sub-actions. Therefore, the energy demand of tool changing (off→on) can be calculated as:

$$E_{TCA} = \sum_{k=1}^{K_{\Delta p}} E_{TC_{\Delta pk}} \tag{19}$$

where E_{TCA} is energy demand of tool changing (off→on), J; $E_{TC_{\Delta pk}}$ is energy demand of power peak caused by sub-action k when the rotating position number of the turret is Δp, J; $K_{\Delta p}$ is the number of power peaks when the rotating position number of the turret is Δp; $E_{TC_{\Delta pk}}$ can be obtained by experimental measurement combined with the statistical analysis method.

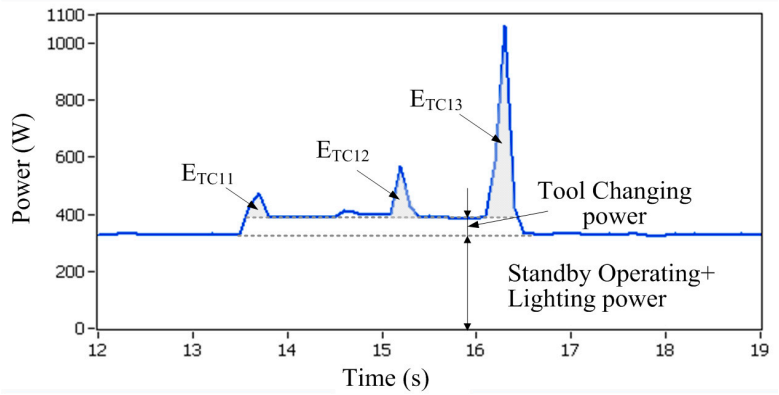

Figure 9. Power curve of tool changing (off→on).

Generally, the rotation method of turret of CNC lathe is the unidirectional tool changing order. Hence, the rotating position number of the turret Δp can be calculated as:

$$\Delta p = \begin{cases} T_{pt} - T_{pi} & , T_{pt} \geq T_{pi} \\ T_p - \left| T_{pt} - T_{pi} \right| & , T_{pt} < T_{pi} \end{cases} \tag{20}$$

where T_{pi} is the initial position of the turret; T_{pt} is the target position of the turret; T_p is the total posts of the turret.

4. Case Study

4.1. Description of State Transition Cases

Case studies of spindle rotation (Ls→Hs), positioning (Ls→Hs), cooling (off→on) and tool changing (off→on) were carried out to show the feasibility of the proposed method. The state transition

cases were performed on a CK6153*i* CNC lathe, with a spindle speed range of 30~2000 r/min, and rapid-positioning speeds of X, Z-axes at 6000, 10,000 mm/min, respectively. In order to compare the forecast energy demand of state transition with the actual energy consumption value, an energy acquisition system was set up by our research group [12]. As shown in Figure 10, the current sensor and voltage sensor are connected with the CNC machine tool to obtain the current and voltage signal and collect the real-time data through two NI-9215 data acquisition cards. The power and energy information of the CNC machine tool are obtained by using LabVIEW software before being stored in the Server SQL database. The sampling interval of the energy acquisition system was set to 0.1 s.

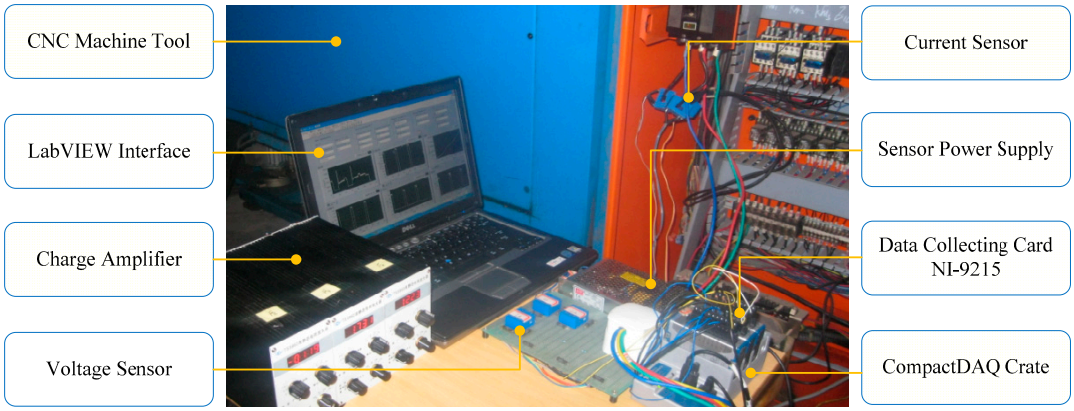

Figure 10. Experimental setup of energy acquisition system.

Based on the modeling method proposed in Section 3, case studies of six state transitions were carried out on the CK61563*i* CNC lathe. The determining process of experimental cases is shown in Figure 11. The principle is that the cases should cover all types of key state transitions. For the state transition spindle rotation (Ls→Hs), two conditions should be considered: initial spindle speed is zero and initial spindle speed is not zero. Therefore, spindle rotation (Ls→Hs)-[0→750 r/min] and (Ls→Hs)-[500→1000 r/min] were selected for the state transition positioning (Ls→Hs), due to the fact that only two feeding directions can be applied for the CNC lathe (X-axis and Z-axis direction). Hence, positioning-Z-axis-[0→10,000 mm/min] and positioning-X-axis [0→6000 mm/min] were selected as experimental cases. For the state transition cooling (off→on), only one condition should be considered: cooling device is transiting from "off" state to "on" state (cooling (off→on) was selected). For the state transition tool changing (off→on), the cutting tool changes from one position of the turret to another. The most commonly used changing was selected: tool changing (off→on)-[T_{pi} = 1, T_{pt} = 2].

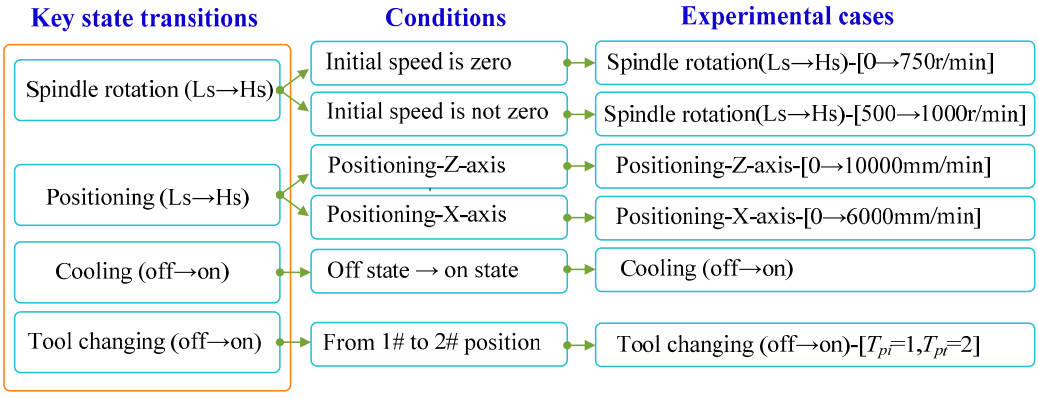

Figure 11. Determining process of experimental cases.

The above-mentioned six cases cover all the four type of key state transitions, and the main parameters of the above cases are shown in Table 1.

Table 1. Main parameters of state transition cases.

State Transition	Main Parameters		
	Initial Parameter	**Target Parameter**	**Supporting Therbligs**
Spindle rotation (Ls→Hs) 0→750 r/min	n_1 = 0 r/min	n_2 = 750 r/min	standby operating/lighting
Spindle rotation (Ls→Hs) 500→1000 r/min	n_1 = 500 r/min	n_2 = 1000 r/min	standby operating/lighting
Positioning (Ls→Hs) Z-axis	v_{rmin} = 0 mm/min	v_{rmax} = 10,000 mm/min	standby operating/lighting
Positioning (Ls→Hs) X-axis	v_{rmin} = 0 mm/min	v_{rmax} = 6000 mm/min	standby operating/lighting
Cooling (off→on)	Off state	On state	standby operating/lighting
Tool changing (off→on)	T_{pi} = 1	T_{pt} = 2	standby operating/lighting

Taking spindle rotation (Ls→Hs)-[500→1000 r/min] as an example, coefficients T_S and α of the AH transmission chain can be obtained according to spindle startup experiment (T_S = 28.42 N·m, α = 39.78 rad/s^2) [33]. The coefficient values are substituted into (3) and (4) to obtain the expressions of the spindle speedup power P_{SR1} and the duration from spindle rotation start to peak power t_{SR1} for the researched CK61563*i* CNC lathe.

$$P_{SR1} = P_{SR}(n_1 + 380t) + 2.98n_1 + 1130.7t(0 < t \leq t_{SR1}) \tag{21}$$

$$t_{SR1} = 0.002632(n_2 - n_1) \tag{22}$$

The duration from peak power to stable power t_{SR2} is related to the target spindle speed n_2. Based on the measured t_{SR2} at different target spindle speeds n_2 (see Table 2), linear regression between t_{SR2} and n_2 is conducted (as shown in Figure 12) to establish the duration model from peak power to stable power (Equation (23)).

$$t_{SR2} = 0.037 + 1.471 \times 10^{-4} n_2 \ (\mathrm{R}^2 = 0.9479) \tag{23}$$

The correlation coefficient is R^2 = 0.9479, which indicates that the established model can well describe t_{SR2} under different target spindle speeds.

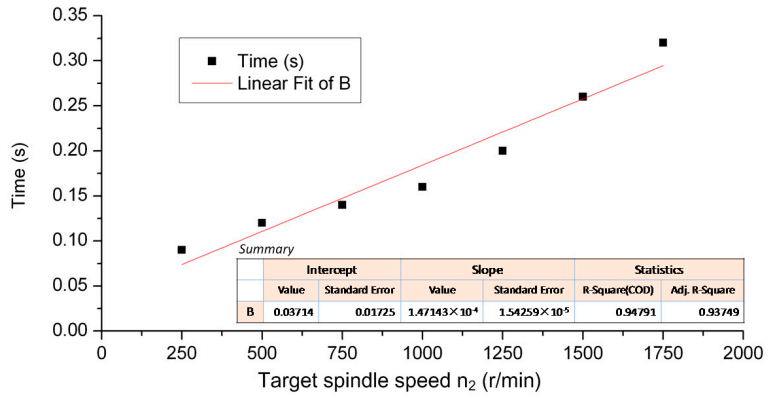

Figure 12. Linear fitting between t_{SR2} and n_2.

Table 2. Duration from peak power to stable power (t_{SR2}) under different target spindle speeds.

Target Spindle Speed n_2 (r/min)	t_{SR2} (s)
250	0.09
500	0.12
750	0.14
1000	0.16
1250	0.20
1500	0.26
1750	0.32

Taking spindle rotation (Ls→Hs) as an example, the known information is the initial speed $n_1 = 0$ r/min and target speed $n_2 = 750$ r/min. Based on the proposed method in Section 3.1, the energy demand of spindle rotation (Ls→Hs)-[0→750 r/min] (E_{SRA}) can be calculated, as shown in Figure 13. The input data, reference equations and calculation results of intermediate variables are clearly shown in this figure.

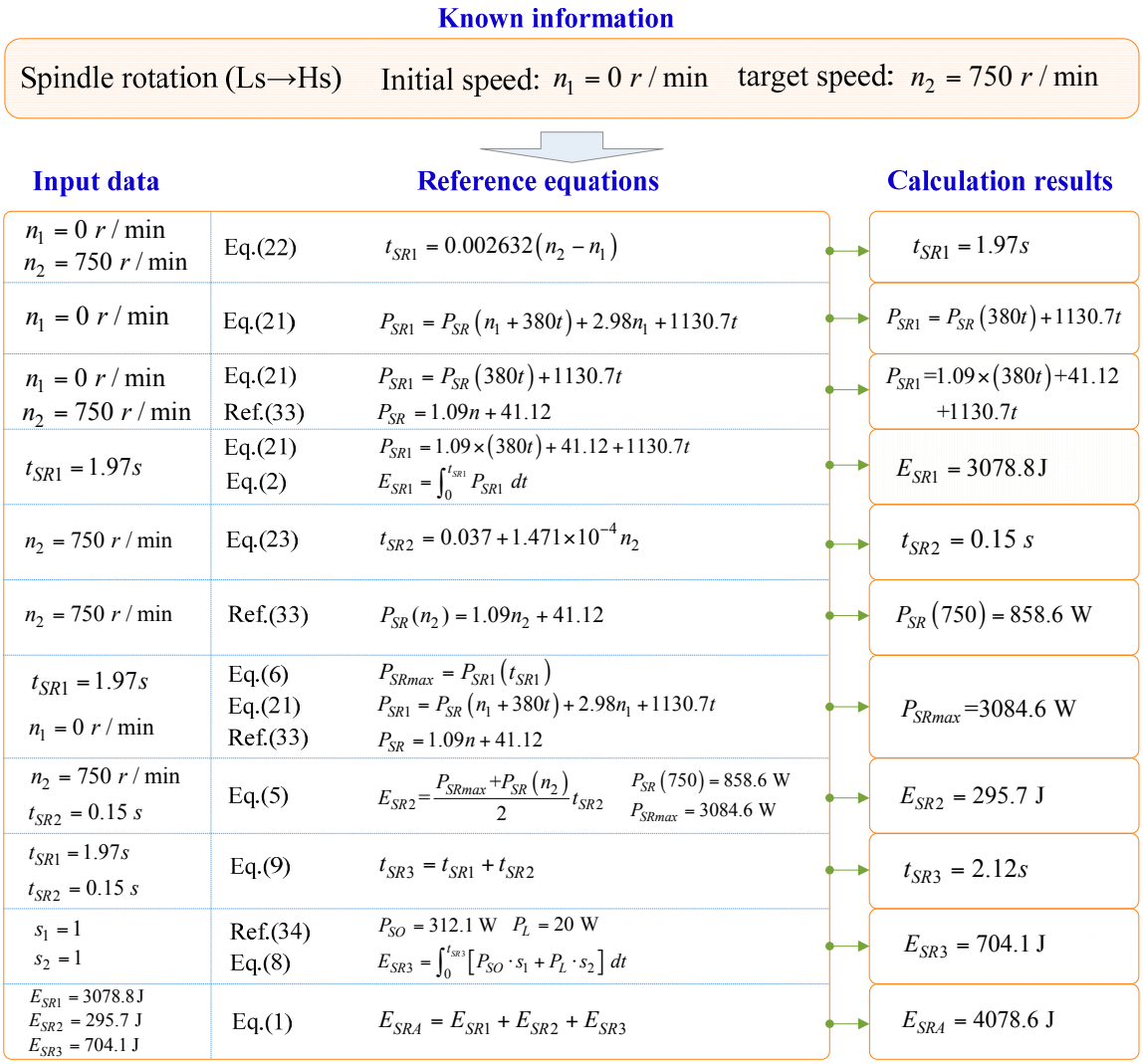

Figure 13. Calculation process of energy demand of spindle rotation (Ls→Hs)-[0→750 r/min].

Similarly, energy demands of the other five state transitions can also be computed according to the established models in Section 3. The obtained energy demands of state transitions-spindle rotation (Ls→Hs)-[0→750 r/min], state transitions-spindle rotation (Ls→Hs)-[500→1000 r/min], positioning (Ls→Hs)-[Z-axis], positioning (Ls→Hs)-[X-axis], cooling (off→on) and tool changing (off→on) are 4078.6 J, 5056.8 J, 277.5 J, 117.2 J, 241.3 J and 116.8 J, respectively.

4.2. Discussion

By using the energy acquisition system shown in Figure 10, the actual energy consumptions of these six state transitions were measured. The predicted energy demand values of these six state transitions are compared to the measured energy values, as shown in Figure 14. It can be seen that most predictive accuracies of the state transition cases are above 90%, which shows that the proposed energy demand models of key state transitions can well describe the energy consumption behaviors of the state transitions of turning processes.

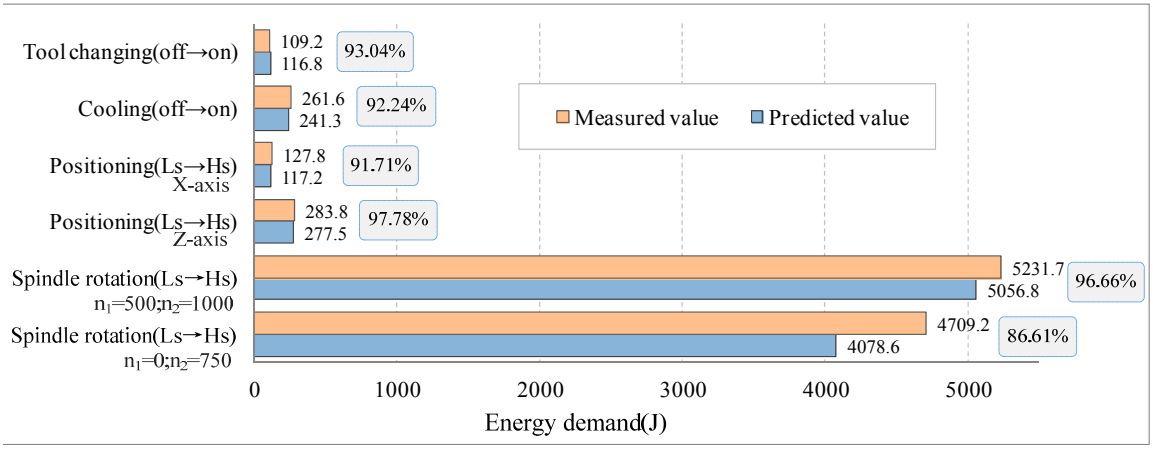

Figure 14. Predicted energy values vs. measured values of state transitions.

For the state transition spindle rotation (Ls→Hs), sometimes average machining power of state transition was used to calculate the energy consumption during state transition. Compared to the model without considering the energy demand of state transitions, the accuracy can be improved to a certain extent via applying the average machining power of state transitions. However, the accuracy of the average power model is not optimistic as this is a simplistic model. The energy demand models proposed in this paper can further improve the energy predictive accuracy of the state transitions compared with the average power model. Taking the state transition spindle rotation (Ls→Hs)-[0→750 r/min] of CK6153*i* as an example, the energy demand of spindle (Ls→Hs)-[0→750 r/min] has been obtained based on the proposed model in this paper by the aforementioned calculating processes: $E_{SRA} = 4078.6$ J (briefly shown in Figure 15). Moreover, if the average power model is used to predict energy consumption, the calculating process and result is also shown in Figure 15. It can be seen that the energy demand of the state transition spindle rotation (Ls→Hs)-[0→750 r/min] calculated by using the average power model is $E_{SRA} = 2524.3$ J. Similarly, predicted energy values with the average power model and this paper's model can be calculated from the state transition spindle rotation (Ls→Hs)-[500→1000 r/min]. The comparison of the predicted energy values with these two models for the state transition spindle rotation (Ls→Hs) is shown in Figure 16.

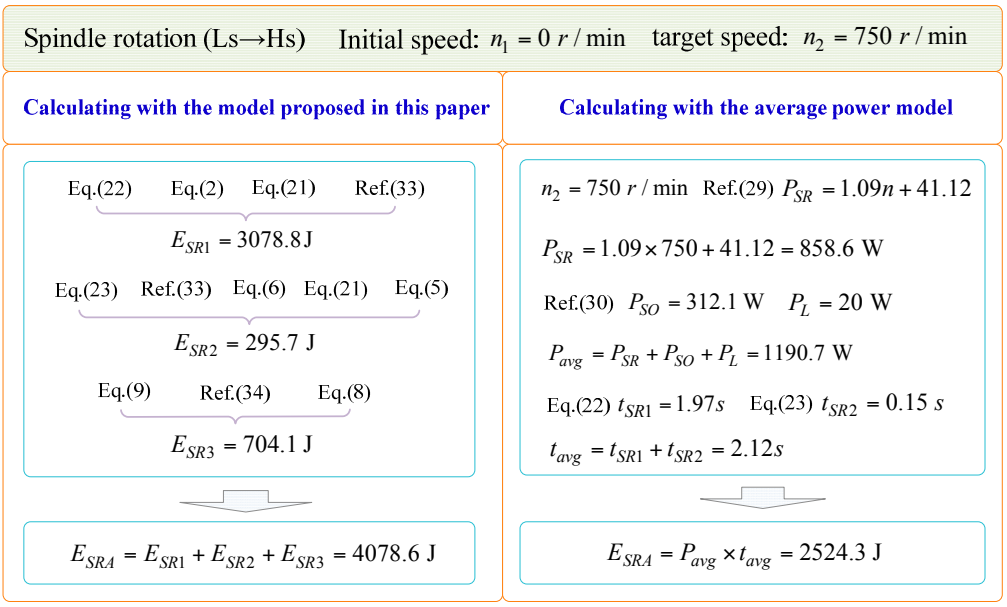

Figure 15. Energy demand calculated with the model proposed in this paper and the average power model.

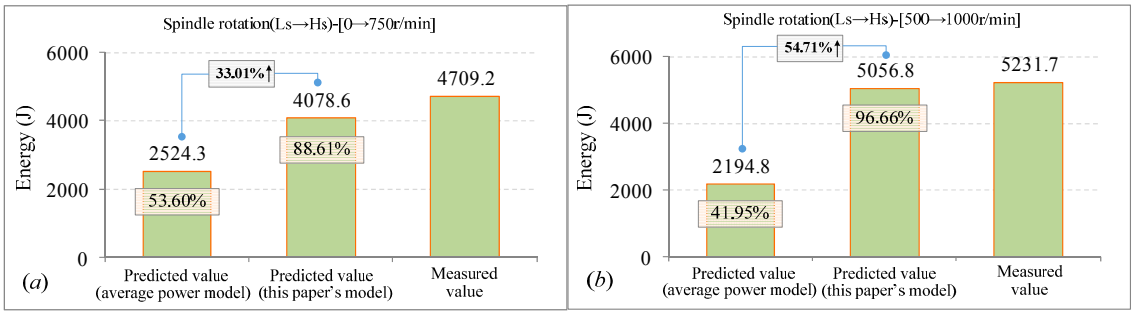

Figure 16. Comparison of predicted values and measured values for (**a**) spindle rotation (Ls→Hs)-[0→750 r/min] and (**b**) spindle rotation (Ls→Hs)-[500→1000 r/min].

It can be seen from Figure 16a that the predicted energy value with the average power model for the state transition spindle rotation (Ls→Hs)-[0→750 r/min] is 2524.3 J (the actual measured energy value is 4709.2 J); the predictive accuracy is thus only 53.60% when using the average power model. When it comes to the state transition spindle rotation (Ls→Hs)-[500→1000 r/min], the predictive accuracy is also not satisfactory (41.95%). The reason is that the power during state transition is treated as a single value in the average power model and the dynamic power change and power peak were not considered. Indeed, the average power is far less than the peak power of the state transition, particularly in the state transition spindle rotation (Ls→Hs). With the proposed method in this paper, the predicted energy value for the state transition spindle rotation (Ls→Hs)-[0→750 r/min] is 4078.6 J. Hence, the predictive accuracy is 88.61%, improving the accuracy by 33.01% compared with the average power model. A similar result is also obtained in the case of the state transition spindle rotation (Ls→Hs)-[500→1000 r/min]. The predictive accuracy is raised from 41.95% to 96.66%, i.e., 54.71% improvement is achieved. The results show that the energy demand model proposed in this paper can further improve the energy-predictive accuracy of the state transitions compared with the average power model.

5. Conclusions

State transitions occur frequently during the turning process, and energy demand of the machining state transition is an important part of that entire process. The establishment of energy demand models of the key state transitions could significantly improve the accuracy of a turning process energy model. The state transitions are classified according to energy characteristics, and the key state transitions for turning processes are identified. Then, the energy demand model of four types of key state transitions are respectively researched and established. Finally, experimental studies and case studies are performed on a CK6153*i* CNC lathe, the results showing that predictive accuracy with the proposed method is generally above 90% for the state transition cases. In particular, the predictive accuracy can be improved by 33.01% and 54.71% for the two state transition cases (spindle rotations (Ls→Hs)-[0→750 r/min] and (Ls→Hs)-[500→1000 r/min]) compared with the average power model. The proposed method in this paper can provide more accurate energy models and reliable data of state transitions for energy optimization of turning processes.

Although this study presents energy demand modeling of key state transitions of the turning process, the dynamic distribution of key state transitions and total energy demand of state transitions throughout the machining process have not yet been investigated. Further research will be carried out to analyze key state transition distribution during the machining process and propose an energy demand modeling method of state transitions for all stages of the machining process.

Acknowledgments: The authors sincerely thank editors and anonymous reviewers for their helpful suggestions on the quality improvement of our paper. This research is supported by the Shandong Provincial Natural Science Foundation, China (No. ZR2016GQ11), Scientific Research Foundation of Shandong University of Science and Technology for Recruited Talents (No. 2015RCJJ049).

Author Contributions: Qinghe Yuan and Dawei Ren proposed the paper structure, Shun Jia and Jingxiang Lv designed and performed the experiments. Shun Jia conceived the paper, analyzed the data and wrote the paper.

Conflicts of Interest: The authors declare no conflict of interest.

Nomenclature

a_f	acceleration in feed table (mm/s^2)
a_p	depth of cut (mm)
d_f	deceleration of feed table (mm/s^2)
E_{CFA}	energy demand of cooling (off→on) (J)
E_{CF1}	energy demand of cooling device during cooling (off→on) (J)
E_{CF2}	energy demand of supporting therblig during(off→on) (J)
E_{FA}	energy demand of positioning (Ls→Hs) (J)
E_{F1}	energy demand of feeding system during positioning (Ls→Hs) (J)
E_{F2}	energy demand of supporting therblig during positioning (Ls→Hs) (J)
E_{SRA}	energy demand of spindle rotation (Ls→Hs) (J)
E_{SR1}	energy demand of spindle system from spindle rotation start to peak power (J)
E_{SR2}	energy demand of spindle system from peak power to stable power (J)
E_{SR3}	energy demand of supporting therbligs during spindle rotation (Ls→Hs) (J)
E_{TCA}	energy demand of tool changing (off→on) (J)
$E_{TC_{\Delta pk}}$	energy demand of power peak caused by sub-action k when the rotating position number of the turret is Δp(J)
IEA	International Energy Agency
$K_{\Delta p}$	number of power peak when the rotating position number of the turret is Δp
L_f	feeding distance (mm)
L_{f0}	critical feeding distance (mm)
LCA	Life Cycle Analysis
n	spindle speed (r/min)
n_1	initial spindle speed (r/min)
n_2	target spindle speed (r/min)

$\vec{OP}$	power vector of forward-operating state
$\vec{OS}$	state vector of forward-operating state
P_{CC}	power of therblig-chip conveying (W)
P_{CFS}	power of therblig-cutting flood spraying (W)
$P_{F1}(t)$	power function of feeding system during positioning (Ls→Hs)
P_L	power of therblig- lighting (W)
P_{MC}	power of therblig- material cutting (W)
P_{SO}	power of therblig-standby operating (W)
P_{SR}	spindle power (W)
P_{SR1}	power of spindle system from spindle rotation start to peak power (W)
P_{SRmax}	power peak of spindle speedup (W)
P_{TC}	power of therblig-tool changing (W)
P_{TS}	power of therblig-tool selecting (W)
P_{XF}	power of therblig-X-axis feeding (W)
P_{YF}	power of therblig-Y-axis feeding (W)
P_{ZF}	power of therblig-Z-axis feeding (W)
s_i	logical representations for *i*th type of therbligs
t_{CF}	transfer time of cooling (off→on) process (s)
t_F	transfer time of positioning (Ls→Hs) (s)
t_{SR1}	duration from spindle rotation start to peak power (s)
t_{SR2}	duration from peak power to stable power (s)
t_{SR3}	duration of spindle rotation (Ls→Hs) (s)
T_p	total posts of the turret
T_{pi}	initial position of the turret
T_{pt}	target position of the turret
T_s	equivalent acceleration torque of spindle (N·m)
v_{f0}	initial feed speed (mm/min)
v_{f1}	maximum feed rate (mm/min)
v_{rmax}	maximum feeding speed of feed table (mm/min)
α	angular acceleration of spindle (rad/s^2)
ω_s	angular velocity of spindle rotation (rad/s)
Δp	rotating position number of the turret

References

1. International Energy Agency. *Energy Technology Perspectives 2010: Scenarios and Strategies to 2050*; International Energy Agency: Paris, France, 2010.
2. Wei, W.; Liang, Y.; Liu, F.; Mei, S.; Tian, F. Taxing strategies for carbon emissions: A bilevel optimization approach. *Energies* **2014**, *7*, 2228–2245. [CrossRef]
3. Thollander, P.; Palm, J. Industrial energy management decision making for improved energy efficiency—Strategic system perspectives and situated action in combination. *Energies* **2015**, *8*, 5694–7703. [CrossRef]
4. Anderberg, S.E.; Kara, S.; Beno, T. Impact of energy efficiency on computer numerically controlled machining. *Proc. Inst. Mech. Eng. B J. Eng.* **2010**, *224*, 531–541. [CrossRef]
5. Brown, N.; Greenough, R.; Vikhorev, K.; Khattack, S. Precursor to using energy data as a manufacturing process variable. In Proceedings of the 6th IEEE International Conference on Digital Ecosystems Technologies (DEST), Campione d'Italia, Italy, 18–20 June 2012.
6. Shao, G.; Kibira, D.; Lyons, K. A virtual machining model for sustainability analysis. In Proceedings of the ASME 2010 International Design Engineering Technical Conferences & Computers and Information in Engineering Conference, Montreal, QC, Canada, 15–18 August 2010.
7. Zulaika, J.J.; Dietmair, A.; Campa, F.J.; López de Lacalle, L.N.; Verbeeten, W. Eco-efficient and Highly Productive Production Machines by Means of a Holistic Eco-Design Approach. In Proceedings of the 3rd Conference on Eco-Efficiency, Egmond an Zee, The Netherlands, 9–11 June 2010.
8. Salonitis, K. Energy efficiency assessment of grinding strategy. *Int. J. Energy Sect. Manag.* **2015**, *9*, 20–37. [CrossRef]

9. Salonitis, K.; Vidon, B.; Chen, D. A decision support tool for the energy efficient selection of process plans. *Int. J. Mech. Manuf. Syst.* **2015**, *8*, 63–83. [CrossRef]
10. Gutowski, T. Energy and Environmental Issues for Manufacturing Processes. Available online: http://web.mit.edu/2.810/www/lecture2011/Environment.pdf (accessed on 27 August 2011).
11. Gutowski, T.; Dahmus, J.; Thiriez, A. Electrical energy requirements for manufacturing processes. In Proceedings of the 13th CIRP International Conference on Life Cycle Engineering, Leuven, Belgium, 31 May–2 June 2006.
12. Jia, S.; Tang, R.Z.; Lv, J.X. Therblig-based energy demand modeling methodology of machining process to support intelligent manufacturing. *J. Intell. Manuf.* **2014**, *25*, 913–931. [CrossRef]
13. Lv, J.X.; Tang, R.Z.; Jia, S. Therblig-based energy supply modeling of CNC machine tools. *J. Clean. Prod.* **2014**, *65*, 168–177. [CrossRef]
14. Li, W.; Kara, S. An empirical model for predicting energy consumption of manufacturing processes: A case of turning process. *Proc. Inst. Mech. Eng. B J. Eng.* **2011**, *225*, 1636–1646. [CrossRef]
15. Balogun, V.A.; Mativenga, P.T. Modeling of direct energy requirements in mechanical machining processes. *J. Clean. Prod.* **2013**, *41*, 179–186. [CrossRef]
16. Jia, S.; Tang, R.Z.; Lv, J.X.; Zhang, Z.W.; Yuan, Q.H. Energy modeling for variable material removal rate machining process: An end face turning case. *Int. J. Adv. Manuf. Technol.* **2016**, *85*, 2805–2818. [CrossRef]
17. Zobel, T.; Malmgren, C. Evaluating the management system approach for industrial energy efficiency improvements. *Energies* **2016**, *9*, 774. [CrossRef]
18. Tan, X.C.; Wang, Y.Y.; Gu, B.H.; Mu, Z.K.; Yang, C. Improved methods for production manufacturing processes in environmentally benign Manufacturing. *Energies* **2011**, *4*, 1391–1409. [CrossRef]
19. Chiu, T.-Y.; Lo, S.-L.; Tsai, Y.-Y. Establishing an integration-energy-practice model for improving energy performance Indicators in ISO 50001 energy management systems. *Energies* **2012**, *5*, 5324–5339. [CrossRef]
20. Peng, T.; Xu, X. Energy-efficient machining systems: A critical review. *Int. J. Adv. Manuf. Technol.* **2014**, *72*, 1389–1406. [CrossRef]
21. Salonitis, K.; Ball, P. Energy efficient manufacturing from machine tools to manufacturing systems. *Procedia CIRP* **2013**, *7*, 634–639. [CrossRef]
22. Salonitis, K.; Zeng, B.; Mehrabi, H.A.; Jolly, M.R. The challenges for energy efficiency casting processes. *Procedia CIRP* **2016**, *40*, 24–29. [CrossRef]
23. Domingo, R.; Marín, M.; Claver, J.; Calvo, R. Selection of cutting inserts in dry machining for reducing energy consumption and CO_2 emissions. *Energies* **2015**, *8*, 13081–13095. [CrossRef]
24. Zhai, Q.; Cao, H.; Zhao, X.; Yuan, C. Cost benefit analysis of using clean energy supplies to reduce greenhouse gas emissions of global automotive manufacturing. *Energies* **2011**, *4*, 1478–1494. [CrossRef]
25. Campatelli, G.; Lorenzini, L.; Scippa, A. Optimization of process parameters using a Response Surface Method for minimizing power consumption in the milling of carbon steel. *J. Clean. Prod.* **2014**, *66*, 309–316. [CrossRef]
26. Santos, J.P.; Oliveira, M.; Almeida, F.G.; Pereira, J.P.; Reis, A. Improving the environmental performance of machine-tools: Influence of technology and throughput on the electrical energy consumption of a press-brake. *J. Clean. Prod.* **2011**, *19*, 356–364. [CrossRef]
27. Herrmann, C.; Thiede, S. Process chain simulation to foster energy efficiency in manufacturing. *CIRP J. Manuf. Sci. Technol.* **2009**, *1*, 221–229. [CrossRef]
28. Abele, E.; Sielaff, T.; Schiffler, A.; Rothenbücher, S. Analyzing energy consumption of machine tool spindle units and identification of potential for improvements of efficiency. In Proceedings of the 18th CIRP International Conference on Life Cycle Engineering, Braunschweig, Germany, 2–4 May 2011.
29. He, Y.; Liu, F.; Wu, T.; Zhong, F.; Peng, B. Analysis and estimation of energy consumption for numerical control machining. *Proc. Inst. Mech. Eng. B J. Eng.* **2011**, *226*, 255–266. [CrossRef]
30. Reinhart, G.; Reinhardt, S.; Föckerer, T.; Zäh, M.F. Comparison of the Resource Efficiency of Alternative Process Chains for Surface Hardening. In Proceedings of the 18th CIRP International Conference on LCE, Braunschweig, Germany, 2–4 May 2011.
31. Avram, O.I.; Xirouchakis, P. Evaluating the use phase energy requirements of a machine tool system. *J. Clean. Prod.* **2011**, *19*, 699–711. [CrossRef]
32. Shi, J.L.; Liu, F.; Xu, D.J.; Chen, G.R. Decision model and practical method of energy-saving in NC machine tool. *China Mech. Eng.* **2009**, *20*, 1344–1346.

33. Lv, J.X. Research on Energy Supply Modeling of Computer Numerical Control Machine Tools for Low Carbon Manufacturing. Ph.D. Thesis, Zhejiang University, Hangzhou, China, 2014.
34. Jia, S. Research on Energy Demand Modeling and Intelligent Computing of Machining Process for Low Carbon Manufacturing. Ph.D. Thesis, Zhejiang University, Hangzhou, China, 2014.
35. CK6153i Series. *Manual Specification of CK6153i Series CNC Lathe*; Jinan First Machine Tool Group Co., Ltd. of China: Jinan, China, 2000.
36. China Commodity Net. Technological Development and Gap of Domestic CNC Machine Tools. Available online: http://ccn.mofcom.gov.cn/spbg/show.php?id=12952 (accessed on 26 April 2012).